PROTEINS
STRUCTURE ■ FUNCTION ■ BIOINFORMATICS

Conformational analysis and design of cross-strand disulfides in antiparallel β-sheets

S. Indu,[1] V. Kochat,[1] S. Thakurela,[1] C. Ramakrishnan,[1] and Raghavan Varadarajan[1,2]*

[1] Molecular Biophysics Unit, Indian Institute of Science, Bangalore, Karnataka, India

[2] Chemical Biology Unit, Jawaharlal Nehru Center for Advanced Scientific Research, Bangalore, Karnataka, India

ABSTRACT

Cross-strand disulfides bridge two cysteines in a registered pair of antiparallel *β*-strands. A nonredundant data set comprising 5025 polypeptides containing 2311 disulfides was used to study cross-strand disulfides. Seventy-six cross-strand disulfides were found of which 75 and 1 occurred at non-hydrogen-bonded (NHB) and hydrogen-bonded (HB) registered pairs, respectively. Conformational analysis and modeling studies demonstrated that disulfide formation at HB pairs necessarily requires an extremely rare and positive χ^1 value for at least one of the cysteine residues. Disulfides at HB positions also have more unfavorable steric repulsion with the main chain. Thirteen pairs of disulfides were introduced in NHB and HB pairs in four model proteins: leucine binding protein (LBP), leucine, isoleucine, valine binding protein (LIVBP), maltose binding protein (MBP), and Top7. All mutants LIVBP T247C V331C showed disulfide formation either on purification, or on treatment with oxidants. Protein stability in both oxidized and reduced states of all mutants was measured. Relative to wild type, LBP and MBP mutants were destabilized with respect to chemical denaturation, although the sole exposed NHB LBP mutant showed an increase of 3.1°C in T_m. All Top7 mutants were characterized for stability through guanidinium thiocyanate chemical denaturation. Both exposed and two of the three buried NHB mutants were appreciably stabilized. All four HB Top7 mutants were destabilized ($\Delta\Delta G^0$ = −3.3 to −6.7 kcal/mol). The data demonstrate that introduction of cross-strand disulfides at exposed NHB pairs is a robust method of improving protein stability. All four exposed Top7 disulfide mutants showed mild redox activity.

Proteins 2011; 79:244–260.
© 2010 Wiley-Liss, Inc.

Key words: cross-strand disulfides; NHB and HB registered pairs; MODIP; torsion angle; chemical denaturation; thermostability.

INTRODUCTION

The role of disulfides in protein stability is well known.[1] Disulfides confer stability by reducing the conformational entropy of denatured state.[2] Removal of naturally occurring disulfides in proteins is accompanied by protein destabilization.[3,4] However, engineering stabilizing disulfides is still a challenge because introduction of disulfides typically does not always result in an increase in stability.[5,6]

It was previously hypothesized that a disulfide cannot be accommodated between residues occurring on adjacent β-strands.[7,8] This hypothesis was supported by the absence of such disulfides in early versions of the protein database.[7,8] However, later surveys revealed that disulfides bridging adjacent β-strands do exist.[9–12] These disulfides linking cysteine pairs on a registered pair on adjacent strands are referred to as cross-strand disulfides. Owing to the two types of registered pairs that can exist in antiparallel β-strands, there are two kinds of cross-strand disulfides occurring either in the non-hydrogen-bonded (NHB) registered pairs or hydrogen-bonded (HB) registered pairs, respectively [Fig. 1(A)].

Cross-strand disulfides occur in proteins of varied folds and functions. Cross-strand disulfides are believed to be highly strained disulfides.[11] The strained nature of the cross-strand disulfides is believed to help these disulfides act as redox switches.[11,13,14] Indeed, it has been shown that, although the majority of disulfides are structurally inert in proteins, there are several disulfides that act as redox-sensitive regulators.[15,16] The oxidation status of cross-strand disulfides is believed to be important for the activity of toxins.[17–19] Conserved cross-strand disulfides occurring in viral fusion proteins and surface glycoproteins are believed to play a role in viral entry.[20–24] The cross-strand disulfide in the D2 domain of CD4 is important in human immunodeficiency virus entry.[25] The redox state of the

Additional Supporting Information may be found in the online version of this article.

Abbreviations: CD, circular dichroism; CGH 10, 10 mM sodium citrate, 10 mM glycine, and 10 mM HEPES; DTT, dithiothreitol; Gdm Cl, guanidinium chloride; Gdm SCN, guanidinium thiocyanate; HB, hydrogen-bonded; IPTG, isopropyl-thio-b-D-galactosidase; LBP, leucine binding protein; LIVBP, leucine, isoleucine, valine binding protein; MBP, maltose binding protein; NHB, non-hydrogen-bonded; PDB, protein data bank; Trx, thioredoxin; WT, wild type.

Grant sponsors: Department of Biotechnology, Government of India and Department of Science and Technology, Government of India

*Correspondence to: R. Varadarajan, Molecular Biophysics Unit, Indian Institute of Science, Bangalore 560 012, Karnataka, India. E-mail: varadar@mbu.iisc.ernet.in.

Received 24 July 2010; Revised 30 August 2010; Accepted 9 September 2010
Published online 22 September 2010 in Wiley Online Library (wileyonlinelibrary.com).
DOI: 10.1002/prot.22878

© 2010 WILEY-LISS, INC.

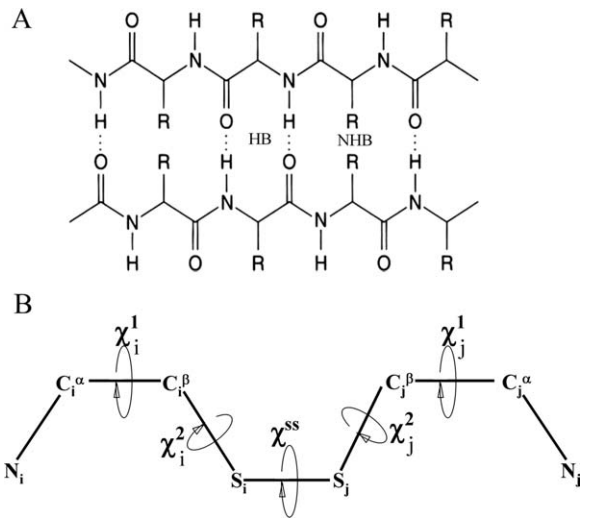

Figure 1

A: NHB (non-hydrogen-bonded) and HB (hydrogen-bonded) registered pairs in an antiparallel β-sheet. **B:** Schematic representation of torsion angles across disulfide bond.

cross-strand disulfide in proteins such as the chaperone PapD[26] and tissue factor[27] determines the activity of the protein. In *Escherichia coli*, the functional disulfide in the oxidoreductase DsbD is a cross-strand disulfide.[28]

In this work, we have studied cross-strand disulfides occurring in registered pairs of antiparallel β-sheets. In an earlier study,[6] we have shown that in antiparallel pairs of β-strands, cross-strand disulfides occur exclusively at NHB pairs; however, there was no obvious explanation for this preference. In addition, we have used thioredoxin (Trx) as a model system to study the effects of introducing disulfides in NHB and HB registered pairs. These studies, which examined four different pairs of sites in Trx, showed that disulfides in NHB positions were stabilizing, whereas those in HB positions were destabilizing.[6] We have now carried out a comprehensive analysis of stereochemical characteristics of cross-strand disulfides. A schematic representation of bonds and torsion angles across a disulfide bond is shown in Figure 1. Modeling studies in conjunction with analysis of protein data bank (PDB) structures were used to understand the stereochemical requirements for formation of cross-strand disulfides. We introduced pairs of CYS at multiple registered pairs in multiple proteins: leucine binding protein (LBP), leucine, isoleucine, valine binding protein (LIVBP), maltose binding protein (MBP), and Top7. The resulting mutants were characterized for disulfide formation, changes in stability to thermal and chemical denaturation, and redox activity.

METHODS

Data set

A nonredundant data set was created from the PDB using the criteria of a minimum resolution of 2.0 Å and a sequence identity cut off of 30%. The nonredundant data set generated has 5025 polypeptides with 2311 disulfides.

Modeling of disulfides by MODIP

Modeling of disulfides was done with the program MODIP, which uses stereochemical criteria described previously.[29,30] Because MODIP requires the coordinates of C^{β} atoms, only non-glycine residue pairs are chosen for modeling of disulfides. The non-glycine residue pairs that satisfy the distance criteria for Cα...Cα (3.8–7.0 Å) and Cβ...Cβ (3.4−4.5 Å) are chosen for geometrical fixation of sulfur atoms. Based on the geometrical parameters of the modeled disulfide, sites are graded in decreasing order of preference for disulfide introduction as A, B, and C.[30]

Energy minimization studies and hydrogen bond detection

Disulfides modeled by MODIP in NHB and HB registered pairs in various proteins were used as starting structures for energy minimization. For registered pairs in proteins, where disulfides were not predicted by MODIP, cysteines were introduced with the mutagenesis tool of SWISS-PDB viewer.[31] Energy minimizations were carried out in vacuum using the l-bfgs minimizer and OPLS-AA/L force field in the GROMACS 3.3.3 package.[32] For all minimizations, convergence was reached within 5000 steps. The hydrogen bonds were detected with HBPLUS.[33]

Chemicals and reagents

Enzyme and dNTPs used for mutagenesis were purchased from NEB. All chemicals used for making buffers and iodoacetamide were purchased from Sigma. Urea, guanidinium thiocyanate (Gdm SCN), guanidinium chloride (Gdm Cl), fast-flow nickel-nitriloacetic acid resin, and Q-sepharose matrices used for protein purification were purchased from GE healthcare.

Mutagenesis, overexpression, and purification

All mutants were made by following the Stratagene QuikChange protocol for site-directed mutagenesis.[34] All mutations were confirmed by DNA sequencing. The pMalp2MBP vector carrying the gene for MBP[35] was used for making the mutant MBP V110C V261C. Both wild type (WT) and mutant MBP proteins were expressed in POP-6590 cells by inducing with 0.1 m*M* isopropyl-thio-β-D-galactosidase (IPTG).[36] The plasmid pKSty carrying the gene for LBP[37] was used for making the mutants LBP L245C Q335C and LBP T247C V333C. The plasmid pJSty carrying the gene for LIVBP[38] was

used for making the mutant LIVBP T247C V331C. LBP and LIVBP mutants were expressed under control of the IPTG-inducible T7 promoter in *E. coli* BL21 (DE3). After growth and induction of *E. coli* at 37°C, purification of MBP, LBP, LIVBP, WT, and mutant proteins was carried out by anion exchange chromatography following chloroform shock as described previously.[39]

The plasmid pET 29b containing the gene for the designed protein Top7 was kindly provided by Prof. David Baker.[40] The mutants made in Top7 were Top7 I4C V23C, Top7 Q5C T22C, Top7 V6C I52C, Top7 V8C I50C, Top7 I10C I48C, Top7 I50C I90C, Top7 S51C T89C, Top7 I52C 88C, and Top7 T82C T89C. Top7 and its mutants were over expressed from a T7 promoter with IPTG induction in BL21 (DE3) cells. Cells were grown in LB media at 37°C to an OD600 of 0.6, induced with 1 m*M* IPTG, and cells were harvested after another 5–8 h of growth at 37°C. After lysis of cells by sonication, the proteins were purified from the soluble fraction by nickel-nitriloacetic acid chromatography.

All purified proteins were dialyzed 10^6-fold against 20 m*M* Tris, 20 m*M* NaCl, pH 8.0. The yields obtained for the MBP, LBP, LIVBP, and Top7 constructs are 40, 20, 20, and 40 mg/L of culture, respectively. All purified proteins were >95% pure as assayed by sodium dodecyl sulfate-polyacrylamide gel electrophoresis. The protein concentrations were determined from absorbance measurements at 280 nm. The extinction coefficients for the WT proteins at 280 nm were determined as described by Pace *et al.*[41] and were 67,000, 38,375, 32,875, and 10,500M^{-1} cm^{-1} for MBP, LBP, LIVBP, and Top7, respectively. For the mutants of MBP, LBP, LIVBP, and Top7 containing a engineered disulfide, the extinction coefficients at 280 nm were determined as described by Pace *et al.*[41] to be 67,125, 38,500, 33,000, and 10,625M^{-1} cm^{-1}, respectively.

In vitro oxidation of proteins

In most cases, disulfides formed spontaneously by air oxidation during protein purification. Where required, disulfide oxidation was facilitated by incubation of protein at a concentration of 15–20 μ*M* with 5 m*M* *o*-phenanthroline and 1.5 m*M* copper sulfate in the buffer 20 m*M* Tris, 20 m*M* NaCl, pH 8.0 at 4°C for 24–48 h.[42] Following oxidation, the proteins were dialyzed 10^6-fold against buffer containing 20 m*M* Tris, 30 m*M* NaCl buffer, pH 8.0 at 4°C.

Iodoacetamide labeling of free cysteines followed by electrospray ionization mass spectrometry

Each of the proteins at a concentration of 30 μ*M* was treated with 100 m*M* iodoacetamide in the presence of 100 m*M* Tris, 3*M* Gdm Cl, pH 8.0 for 4 min at room temperature.[43] In the case of Top7 mutants, the denaturant in the labeling reaction mentioned above was replaced with 4*M* Gdm SCN. After incubation with iodoacetamide, the reaction was quenched with 5% formic acid. The samples were desalted into 0.1% formic acid on a Hi-Trap desalting column (GE-Healthcare). The desalted samples were analyzed by direct injection on a Bruker Daltonics Esquire 3000 plus electrospray ionization mass spectrometer in positive ion mode to determine whether the CYS residues were in the oxidized or reduced state.[5,43]

Circular dichroism measurements

All far UV circular dichroism (CD) spectra were recorded on a Jasco715 spectropolarimeter using a cuvette of path length 1 mm. The recordings for all proteins were made in 20 m*M* Tris, 20 m*M* NaCl, pH 8.0. For obtaining proteins in the reduced state, the protein stocks (40 μ*M* for LBP, LIVBP, and MBP proteins, and 200 μ*M* for Top7 proteins) were incubated for 30 min in reducing denaturant buffer (reducing denaturant buffer for LBP, LIVBP, and MBP proteins is 3*M* urea, 20 m*M* Tris, 20 m*M* NaCl, pH 8.0, 2 m*M* dithiothreitol (DTT) and reducing denaturant buffer for Top7 proteins is 4*M* Gdm SCN, 20 m*M* Tris, 20 m*M* NaCl, pH 8.0, 10 m*M* DTT). After reduction, the protein stocks were diluted 20-fold into 20 m*M* Tris, 20 m*M* NaCl, pH 8.0 buffer containing 1 m*M* DTT. Parameters for spectra collection were 20 nm/min scan rate, 8 s response time, and 2 nm bandwidth. Each spectrum is an average of four scans from 200 to 250 nm. Protein concentration used for MBP, LBP, and LIVBP proteins and their mutants was 2 μ*M* and that for Top7 and its mutants was 10 μ*M*. Buffer spectra were collected under the same conditions and subtracted from the protein spectra.

Chemical denaturation studies

The chemical denaturant used for MBP, LBP, LIVBP proteins, and their mutants was urea. 0.2 μ*M* protein samples were incubated with varying concentrations of urea at 25°C in 20 m*M* Tris, 20 m*M* NaCl, pH 8.0 for 3 h. Top7 is a highly stable protein, which shows a C_m of 6.6*M* when unfolded with Gdm Cl at 25°C.[40] To ensure that all Top7 mutants, including those that are more stable than WT Top7, are completely unfolded during chemical denaturation studies, Gdm SCN, a stronger denaturant was used. Therefore, Top7 and its mutants were incubated with varying concentrations of Gdm SCN at 25°C for 3 h in 20 m*M* Tris, 20 m*M* NaCl, pH 8.0. Protein concentrations used for fluorescence spectra collection are 0.2 μ*M* for all proteins except Top7 (2 μ*M*). Fluorescence emission spectra were recorded for denatured protein samples in 6*M* urea (for MBP, LBP, LIVBP proteins, and their mutants) and 5*M* Gdm SCN (for Top7 and its mutants) in the buffer 20 m*M* Tris, 20 m*M* NaCl, pH 8.0. For obtaining proteins in the reduced state, the protein stocks (20 μ*M* for LBP, LIVBP, and MBP proteins, and 200 μ*M* for Top7 proteins) were

incubated for 30 min in reducing denaturant buffer (reducing denaturant buffer for LBP, LIVBP, and MBP proteins is 3*M* urea, 20 m*M* Tris, 20 m*M* NaCl, pH 8.0, 5 m*M* DTT; and reducing denaturant buffer for Top7 proteins is 4*M* Gdm SCN, 20 m*M* Tris, 20 m*M* NaCl, pH 8.0, 50 m*M* DTT). After reduction, the protein stocks were diluted 100-fold into 20 m*M* Tris, 20 m*M* NaCl, pH 8.0 buffers containing different concentrations of the denaturant and 5 m*M* DTT. All fluorescence spectra were collected on a Fluorolog-3 spectrofluorimeter machine. The samples were excited at 280 nm, and emission spectra were collected in the range of 300–400 nm with 100 nm/min scan rate, medium response time, and excitation and emission slit widths of 2 and 5 nm, respectively. The spectra for each protein collected in the presence and absence of denaturant were compared. Wavelength corresponding to maximum change between folded and denatured protein was chosen for each protein for denaturation studies. At the chosen wavelength for each protein, emission intensities were recorded as a function of denaturant concentration. The data obtained were fitted to a two-state model as described previously.[44]

Thermal denaturation studies

Thermal denaturation studies were carried out on a VP-DSC instrument (Microcal) instrument. Before carrying out differential scanning calorimetry, the proteins were dialyzed 10^6-fold against CGH 10 buffer (a mixture of 10 m*M* sodium citrate, 10 m*M* glycine, and 10 m*M* HEPES buffer), pH 7.0. The protein concentration used was 25 μ*M* for each protein. The studies were carried out in CGH 10 buffer with a scan rate 1°C/min. Two scans were performed in succession to determine the reversibility of the transitions.

Insulin reduction assay

All experiments[45] were carried out at 25°C in a Jasco V-530 spectrophotometer using a 1-cm path length cuvette. Each assay mixture contained 0.1*M* phosphate buffer (pH 7.0), 2 m*M* EDTA, 0.13 m*M* porcine insulin, 0.33 m*M* DTT, and 10 μ*M* of the protein to be studied. Following DTT addition, the formation of insoluble insulin B-chain aggregates was monitored by measurement of the intensity of scattered light at 650 nm as a function of time. The activity of WT Trx was monitored as a positive control. The reaction mixture lacking protein served as negative control.

RESULTS AND DISCUSSION

Identification of antiparallel β-strands and registered pairs

The "SHEET" records of the PDB files in the nonredundant data set were used to identify antiparallel pairs of strands within a β-sheet. The entries in columns 46–69 of the PDB records were used to identify the first pair of registered residues "*i*" and "*j*" in spatially adjacent antiparallel strands of a β-sheet.

For classifying registered pairs as NHB or HB, the two backbone N...O distances, that is, $N_i...O_j$ and $N_j...O_i$ were computed. If the N...O distance lies between 2.4–3.6 Å, then the interaction is considered to be a hydrogen bond. Depending on the existence of 0, 1, or 2 backbone N...O hydrogen bonds, the registered pair is classified as NHB, HB1, or HB2, respectively. The above assignment of registered pairs was repeated for all pairs obtained by moving the position by one residue in opposite directions in the two antiparallel strands till the ends of the strands are reached. A total of 54,207 NHB and 40,886 HB pairs were identified in the nonredundant data set.

Disulfides occurring within antiparallel β-strands

The study of the nonredundant data set showed that there are 90 disulfides, which bridged residues occurring on adjacent strands of an antiparallel β-sheet. These disulfides can be classified into the following two types: (a) Disulfides between nonregistered cysteines occurring on adjacent strands: There are 14 instances of disulfides connecting nonregistered cysteines occurring on adjacent strands. These have been listed in Table SI (Supporting Information). There are 0, 1, and 2 registered pairs between the bridged cysteines in six, six, and two instances, respectively. (b) Disulfides between cysteines on adjacent strands occurring in a registered pair: These disulfides are referred to as cross-strand disulfides and are the most abundant form of disulfides occurring within antiparallel β-sheets. There are 76 examples of cross-strand disulfides of which only one occurs in a HB registered pair (PDB ID: 1b56) (Table SII, Supporting Information). All the remaining disulfides occur in NHB registered pairs. The folds for all the cross-strand disulfides were ascertained from the SCOP database.[46] The two most common folds adopted by proteins with cross-strand disulfides are six-bladed β-propeller (10.7%) and immunoglobulin-like β-sandwich (14.7%). All the proteins with the fold six-bladed β-propeller in our data set are viral surface glycoproteins.[47–50] The proteins with immunoglobulin-like β-sandwich fold include viral surface glycoproteins,[51,52] DsbD,[28] toxins,[18] and eukaryotic cell surface receptors.[53–57] The nonoccurrence of disulfides in HB registered pairs prompted us to examine the entire PDB to ensure that this observation is true of the entire data set. The total number of cross-strand disulfides in the entire PDB is 2576 of which 2570 occur in NHB pairs and six occur in HB pairs. Of the six proteins, the S...S distance for the HB registered pair of cysteines in PDB ID 1jjj is 2.6 Å, although the PDB "SSBOND" record indicates a disulfide between the cysteines occurring at this HB pair. This protein was not considered for further analysis of disulfides occurring at

Table I
Disulfide Preferences for Cysteines in Registered Pairs of Antiparallel Strands[a]

Type of registered pair	I[b]	II[c]	III[d]	IV[e]
NHB	75	15	0	67
HB	1	25	1	20

[a]The analysis uses the nonredundant data set.
[b]Number of cysteines in registered pairs, which are disulfide bonded to each other.
[c]Reduced cysteines in registered pairs.
[d]Cysteines in registered pairs where one of the cysteines is disulfide bonded with a cysteine elsewhere.
[e]Cysteines in registered pairs where both the cysteines are disulfide bonded with cysteines elsewhere.

HB registered pair because of the long S...S distance. The sequences of the remaining five proteins having disulfides in HB registered pairs have a sequence identity >90%. Hence, in the PDB, there is only one nonredundant example of a cross-strand disulfide at a HB registered pair. As discussed previously,[6] this disulfide has an unusual χ^{ss} of 140.4° (disulfide geometry discussed further in the following section). The occurrence of cysteines in registered pairs (Table I) indicates that, although cysteine pairs can occur in HB registered pairs, the formation of disulfide at these positions is almost never observed. In the following sections, we have tried to determine the reasons for this observation.

The nonredundant data set was also examined for the occurrence of disulfides within a single β-strand. No such disulfides were found in our nonredundant data set. However, when the entire PDB was used, nine instances of intrastrand disulfides were found in antiparallel β-sheets. Of these nine, seven are homologous structures sharing sequence identity >90%. The three nonhomologous examples occur in metabotropic glutamate receptor (PDB ID: 1ewk), mitogen-activated kinase kinase kinase (PDB ID: 2irm), and uridylate-specific endoribonuclease (PDB ID: 2ozk). All three instances have a CXC motif. The occurrence of intrastrand disulfides is observed only in CXC motifs because the cysteines in such a motif will have side chains on the same face of the sheet and would be separated by an optimal distance for bridge formation.

Conformations of naturally occurring cross-strand disulfides

Cα...Cα and Cβ...Cβ distances for all residues occurring as registered pairs in the nonredundant data set were computed (Fig. 2). The distance distributions for cross-strand disulfides have significant overlap with those for NHB pairs, but not HB pairs. The HB pairs have larger Cα...Cα distances compared with NHB cysteine pairs. The Cα...Cα and Cβ...Cβ distances for the only HB cross-strand disulfide in our data set is indicated with a filled triangle in Figure 2(C). The Cα...Cα distance for this disulfide is longer than that for NHB cysteine pairs. This difference in Cα...Cα distance may be one contributor to the observed preference of occurrence of such disulfides at NHB pairs.

We next examined the disulfide torsional angle distributions for cross-strand disulfides. Figure 1(B) is a schematic of torsion angles across disulfides. Analysis of the torsion angles for the 75 cases of NHB cross-strand disulfides revealed that all of them have a distinct pattern of torsion angle signs as "−−+−−" for $\chi^1{}_i\chi^2{}_i\chi^{ss}\chi^2{}_j\chi^1{}_j$. The signs "−" and "+" are used for χ when $0^\circ > \chi > -180^\circ$ and $0^\circ \leq \chi \leq 180^\circ$, respectively. Throughout this article, wherever a five-symbol combination is given, it refers to the set of five torsional angles ($\chi^1{}_i\chi^2{}_i\chi^{ss}\chi^2{}_j\chi^1{}_j$),

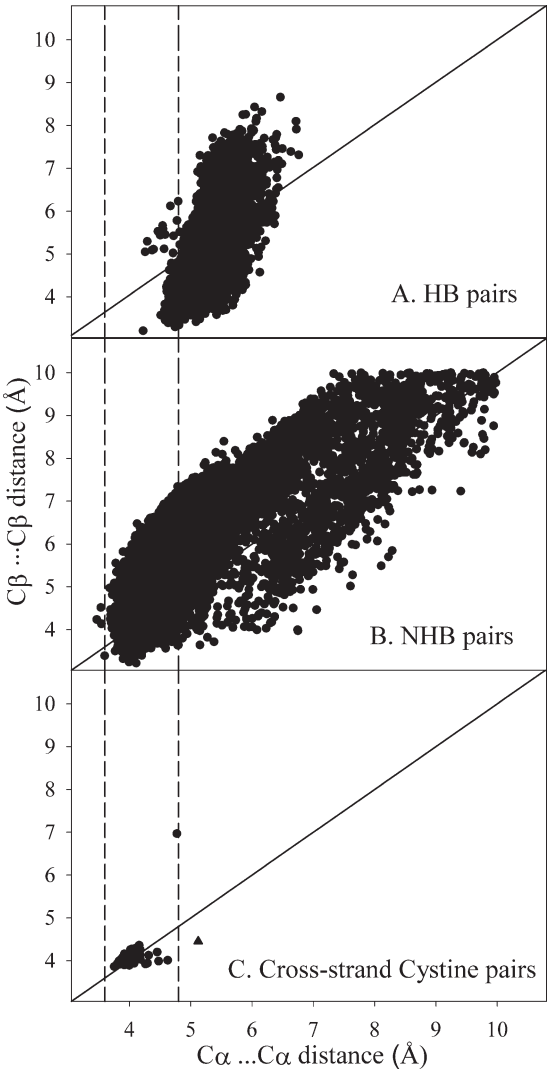

Figure 2
Cα...Cα and Cβ...Cβ distances for (**A**) HB registered pairs, (**B**) NHB registered pairs, and (**C**) cystines in registered pairs occurring in the nonredundant set. The point indicated by a triangle in (C) is for the sole HB cross-strand disulfide in protein with PDB ID 1b56. The dashed lines in the plots enclose the observed range for NHB cystines.

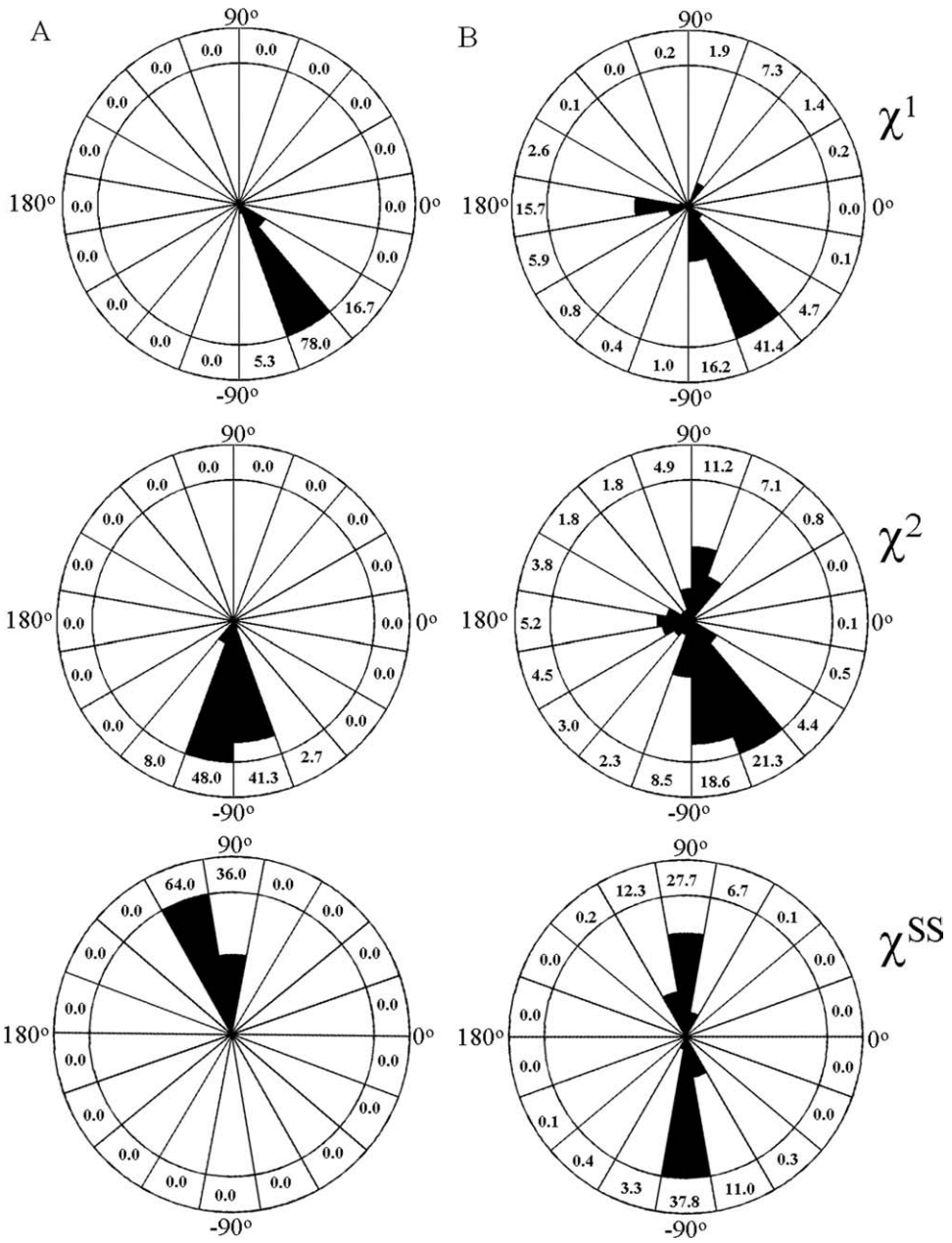

Figure 3

Circular histograms showing the percentage distributions for CYS side chain torsion angles for (**A**) NHB cross-strand disulfides and (**B**) all naturally occurring disulfides. The percentage values for various angle ranges are indicated on the circumference of the histograms.

respectively. It must be noted that the χ^{ss} is positive in all NHB cross-strand disulfides, although χ^{ss} can adopt values around $\pm 90^{\circ}$ for proteins. Conformational analysis of disulfides carried out previously with a data set containing seven NHB cross-strand disulfides also showed that the χ^1 and χ^2 torsion angles adopted values in the range of -30° to -90°, and χ^{ss} in the range of 60–120°.[9] A comparison of torsion angles adopted by cross-strand disulfides versus all naturally occurring disulfides is shown in Figure 3. The torsion angles across disulfides in the five cases of HB cross-strand disulfides occurring in the PDB are listed along with the average values for those in NHB cross-strand disulfides in Table II. In four of the five HB cross-strand disulfides (1b56, 1hre, 1ahk, and 1ahm), at least one of the χ^1 values is positive. The fifth example (1hrf) has both χ^1 values negative. However, one of the χ^1 values is -174.9°, which is very different from the observed χ^1 value for cross-strand disulfides. A comparison of the data in Table II with the distribution of χ values typically found in disulfides (Fig. 3)

Table II
Torsion Angles[a] Across Naturally Occurring Cross-Strand Disulfides

Pair type	PDB ID	Chain ID	Cys_i–Cys_j	$\chi^1{}_i$	$\chi^2{}_i$	χ^{ss}	$\chi^2{}_j$	$\chi^1{}_j$
NHB	All[b]	—	—	−55.8 ± 7.2	−94.6 ± 12.2	102.4 ± 5.8	−90.2 ± 11.4	−59.1 ± 8.8
HB	1b56	A	120–127	**55.6**[c]	−62.8	**140.4**	**115.0**	**96.7**
HB	1hre	A	182–196	−53.1	**162.5**	−63.0	−75.9	175.3
HB	1hrf	A	182–196	**−32.3**	**137.5**	**−56.8**	**−99.7**	−174.9
HB	1ahk	A	8–119	**−31.7**	74.2	**14.9**	**−159.3**	**137.1**
HB	1ahm	A	8–119	**−8.5**	**115.4**	**−41.2**	**−105.7**	**160.8**

[a]All angles are listed in degrees.
[b]The values listed are the average torsion angles across naturally occurring NHB cross-strand disulfides in nonredundant dataset.
[c]The angles that have an occurrence of <10% occurrence in the nonredundant disulfide data set are highlighted in bold (compare with Fig. 3).

clearly demonstrates that the values for the HB disulfides in Table II are atypical. Positive χ^1 values are very rare in naturally occurring disulfides possibly because this results in an unfavorable steric repulsion between the S atom and the carbonyl oxygen. In addition, all the HB disulfides have χ^{ss} values far from the canonical values of $\pm 90^\circ$. In contrast, NHB disulfides have dihedral angles similar to those for other disulfides (compare average values in first row of Table II with distributions in Fig. 3). The backbone torsion angles (ϕ and ψ) of the cysteines forming the NHB cross-strand disulfides have conformations similar to those of residues occurring in strands (Fig. 4), demonstrating that no deviation of the backbone from a typical β-conformation is required for cross-strand disulfide formation.

To understand the occurrence of positive χ^{ss} values in cross-strand disulfides, disulfides were modeled in two proteins (1h4w and 1e8u) with NHB cross-strand disulfides. There are naturally occurring cross-strand disulfides occurring in both 1h4w and 1e8u between CYS A136-CYS A201 and CYS A542-CYS A531, respectively. The value of χ^{ss} for the two disulfides mentioned above is 95.3° and 98.6°, respectively for 1h4w and 1e8u. For each of the disulfides, the χ^1 of at least one of the cysteines involved in the bridge was altered such that it is no longer in the −60° region. The alteration of χ^1 changed the coordinates of the residue's sulfur atom. A disulfide was then modeled by keeping χ^1 fixed at the new value and changing the other disulfide torsion angles. In all cases, where χ^1 was no longer in the −60° region, the modeled disulfide had a negative χ^{ss} value (Table III). Thus, it seems from this limited conformational search that if either $\chi^1{}_i$ or $\chi^1{}_j$ is not in the −60° region, χ^{ss} is likely to adopt a negative value. In antiparallel strands, when a cross-strand disulfide is formed in NHB registered pairs, the most probable value of χ^1 will be in the −60° region, and, consequently, χ^{ss} will be in the +90° region. Furthermore, as can be seen in Figure 3(B), χ^1 values in the −60° region are among the most favorable for all types of disulfides.

Modeling of disulfides by MODIP

To obtain further insight into conformational constraints in cross-strand disulfides, MODIP was used to model disulfides at NHB and HB pairs occurring in the sheets of the nonredundant data set. Only A- and B-grade disulfides predicted by MODIP have been considered for the study. The MODIP results are summarized in Table IV. A total number of 710, 788, and 719 disulfides of A- and B-grades were predicted for NHB, HB_2, and HB_1 pairs, respectively. Among the disulfides modeled for each type of registered pair, the percentages of predicted A-grade disulfides are 37.2%, 3.6%, and 4.0% for NHB, HB_2, and HB_1 pairs, respectively. A-grade modeled disulfides have geometrical parameters similar to that observed in naturally occurring disulfides. This indicates that MODIP favors disulfide prediction more at NHB pairs than HB pairs. The most preferred combination of torsion angles $\chi^1{}_i\chi^2{}_i\chi^{ss}\chi^2{}_j\chi^1{}_j$ for MODIP modeled disulfides at NHB pairs is "−−+−−" (22.5% A-grade and 13.5% B-grade). This is in agreement with the observation that all naturally occurring NHB cross-strand disulfides have sign combination "−−+−−" for the torsion angles. The second most common type of MODIP

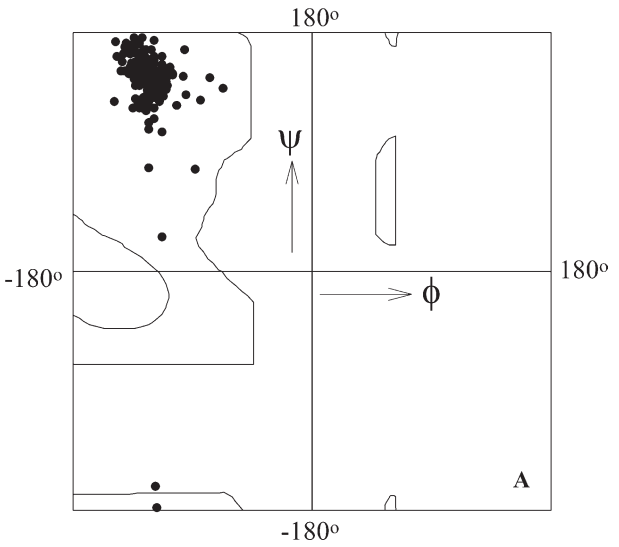

Figure 4
Ramachandran plot for the cystines involved in NHB cross-strand disulfides.

Table III
Modeling of NHB Cross-Strand Disulfide With Altered χ^1 Torsion Angle[a]

PDB ID/chain ID	Bridged Cys, Cys_i–Cys_j	Angle			Angle of rotation		Altered angle		
		$\chi^1{}_i$	$\chi^1{}_j$	χ^{ss}	$\chi^1{}_i$	$\chi^1{}_j$	$\chi^1{}_i$	$\chi^1{}_j$	χ^{ss} of modeled disulfide
1h4w/A	136–201	−51.6	−35.4	95.3	0.0	0.0	−51.6	−35.4	95.3
1h4w/A	136–201	−51.6	−35.4	95.3	−90.0	0.0	−141.6	−35.4	−95.8
1h4w/A	136–201	−51.6	−35.4	95.3	0.0	−90.0	−51.6	−125.4	−85.1
1e8u/A	531–542	−51.2	−68.7	98.6	0.0	0.0	−51.2	−68.7	98.6
1e8u/A	531–542	−51.2	−68.7	98.6	−90.0	0.0	−141.2	−68.7	−85.1
1e8u/A	531–542	−51.2	−68.7	98.6	0.0	−90.0	−51.2	−158.7	−95.8

[a]All angles are listed in degrees.

modeled disulfides at NHB pairs have the sign combination "−−−+−" (11.3% A-grade and 25.6% B-grade). Thus, five examples of the MODIP modeled disulfides with sign combination "−−+−−" and five examples with sign combination "−−−+−" were used for energy minimization studies (discussed in the next section).

The most common type of disulfides modeled at HB pairs is "++−−+" (2.2% A-grade and 72.9% B-grade). It must be noted that both χ^1's for the common MODIP modeled disulfides at HB pairs are positive unlike those for typical naturally occurring disulfides, including NHB cross-strand disulfides. Also, the χ^{ss} angle is negative in contrast to a positive χ^{ss} for NHB cross-strand disulfides.

The above observations suggest that disulfides can be introduced at NHB pairs with reasonable stereochemistry. In contrast, at HB positions, disulfides if formed are likely to be strained.

Energy minimization studies

To ascertain the torsional stress across the disulfides at NHB and HB registered pairs, energy minimizations were carried out with GROMACS version 3.3.3. The following structures were energy minimized:

i. Ten examples of MODIP modeled disulfides at NHB pairs: Five of these predicted disulfides have sign combination "−−+−−," whereas the others had "−−−+−." These conformations were chosen because they are the most common types of MODIP modeled disulfides at NHB pairs.
ii. Eight examples of MODIP modeled disulfides at HB pairs: All the eight modeled disulfides have "++−−+" as their sign combination. This combination of torsion angles across disulfide is the most common form of disulfide modeled by MODIP at HB pairs. Both in (i) above and here, the coordinates of the sulfur atoms for the cystines in the starting structures for the energy minimizations were obtained from the MODIP modeled disulfides.
iii. Energy minimization studies were also carried out for modeled disulfides in four proteins studied experimentally: Top7, LIVBP, LBP, and MBP. Disulfides were introduced at different NHB and HB positions of these proteins for experimental studies (Tables V and VI). The disulfides for proteins Top7 S51C T89C and Top7 T82C T89C were the only cases, where MODIP predicted formation of a disulfide. The MODIP-generated cystine coordinates were used for these two cases for generating the starting structure for energy minimization studies. For the remaining cases, the cysteines were introduced using the mutagenesis tool of Swiss-PDB viewer. In Swiss-PDB viewer, the usage of the mutagenesis tool allows one to choose one of the three rotamers available for cysteine. The rotamers of the two cysteines chosen were such that their combination gave the shortest distance between sulfur atoms of the introduced cysteines.

All protein structures with the modeled disulfides were subjected to energy minimization to obtain further insight into why cross-strand disulfides are preferred at NHB positions and why they adopt the conformation with torsion angle combination $\chi^1{}_i\chi^2{}_i\chi^{ss}\chi^2{}_j\chi^1{}_j$ of "−−+−−" predominantly. The results have been summarized in Table SIII (Supporting Information).

Table IV
Torsion Angles Across MODIP Predicted Cross-Strand Disulfides

Torsion angles[a]	% of MODIP-predicted disulfides for each type of registered pair					
	NHB registered pairs		HB1 registered pairs		HB2 registered pairs	
	A-grade	B-grade	A-grade	B-grade	A-grade	B-grade
+++−+	0.0	0.6	1.1	7.0	0.6	20.1
++−−+	0.1	0.3	2.2	72.9	1.8	56.1
+−++−	1.1	1.0	0.3	2.6	0.3	12.3
−+−+−	1.4	15.9	0.0	0.0	0.0	0.6
−−−+−	11.3	25.6	0.0	0.3	0.0	0.0
−−+−−	22.5	13.5	0.0	0.0	0.0	0.0
Total number of predicted disulfides	264	446	29	690	28	760

[a]The signs of torsion angles across cystine in the order of $\chi^1{}_i\chi^2{}_i\chi^{ss}\chi^2{}_j\chi^1{}_j$. Only those combinations with a frequency of >10% are shown.

Table V
Urea and Thermal (DSC) Denaturation Studies of WT and Mutants of LBP and MBP Proteins Under Oxidized and Reduced Conditions

Protein[a]	Residues mutated to Cys: N-terminal residue (SA[b])	Residues mutated to Cys: C-terminal residue (SA[b])	Pair type[c]	Side chain H-bonds[d]	ΔG^0 (25°C)[e] (kcal/mol)	C_m[f] (M)	$\Delta\Delta G^{0g}$ (25°C) (kcal/mol)	$\Delta\Delta\Delta G^{0h}$ (25°C) (kcal/mol)	ΔC_m (M)	T_m[i] (°C)	ΔT_m (°C)
LBP WT					12.3 ± 2.7	2.9	—	1.4	—	58.9	—
LBP L245C Q335C	L245 (7.2)	Q335 (47.9)	E-NHB	0	10.2 ± 0.2	2.4	−2.1	0.0	−0.5	62.0	3.1
LBP T247C V333C	T247 (0.9)	V333 (5.9)	B-NHB	0	9.4 ± 0.3	2.2	−2.9	>1.6	−0.7	57.3	−1.6
LBP WT[redj]					6.6 ± 0.2	1.5	—	—	—	N.D[k]	N.D
LBP L245C Q335C[red]	L245 (7.2)	Q335 (47.9)	E-NHB	0	4.5 ± 0.9	1.0	−2.1	0.0	−0.5	N.D	N.D
LBP T247C V333C[redl]	T247 (0.9)	V333 (5.9)	B-NHB	0	<2.1 ± 0.2	<0.5	<−4.5	>1.6	<−1.0	N.D	N.D
MBP WT					12.4 ± 1.1	3.6	—	—	—	64.6	—
MBP V110C V261C	V110 (0.1)	V261 (0.0)	B-NHB	0	11.9 ± 0.2	3.4	−0.5	3.0	−0.2	63.4	−1.2
MBP V110C V261C[red]	V110 (0.1)	V261 (0.0)	B-NHB	0	8.9 ± 0.1	2.6	−3.5	3.0	−1.0	N.D	N.D

[a]The mutant LIVBP T247C V331C was not studied because it did not undergo complete oxidation. The percent side chain accessibilities of the residues T247 and V331 in the LIVBP WT structure are 0.1 and 0.0, respectively.
[b]%Side chain accessibilities for WT residue are mentioned in parentheses.
[c]A mutant is referred to as exposed if at least one of the residues of the pair has %side chain accessibility >7%. Types of registered pairs are E-NHB (exposed NHB), B-NHB (buried NHB), E-HB (exposed HB), and B-HB (buried HB).
[d]Number of hydrogen bonds formed by side chains of the WT residues.
[e]The m values used for fitting data for LBP and its mutants in the oxidized and reduced states are -4.2 kcal mol^{-1} M^{-1} and -4.5 kcal mol^{-1} M^{-1}, respectively. The m value used for fitting data for MBP and its mutant in both oxidized and reduced states is -3.4 kcal mol^{-1} M^{-1}.
[f]Approximate error is 0.05M for C_m.
[g]$\Delta\Delta G^0 = \Delta G^0$(mutant) $- \Delta G^0$(WT) where ΔG^0 is free energy of unfolding.
[h]$\Delta\Delta\Delta G^0 = \Delta\Delta G^0$(oxidized) $- \Delta\Delta G^0$(reduced).
[i]Approximate error is 1.0°C for T_m.
[j]All melts in the reduced state were carried out in the presence of 20-fold molar excess of DTT.
[k]Thermal stability of the proteins in the reduced state was not determined (N.D.).
[l]Protein LBP T247C V333C in the reduced state was highly destabilized. Consequently, no folded baseline was obtained during urea denaturation. Approximate parameters of unfolding for this reduced mutant from a two-state fit were derived by using the slope and intercept values of the folded baseline of reduced LBP WT [Fig. 6(A)].

All five NHB-modeled disulfide-containing structures on minimization retained the sign combination of "−−+−−." Further, in all the cases, the change in χ^1 on minimization is <40°, indicating that the χ^1 angles are poised to accommodate the disulfide. Minimization of the structures with NHB-modeled disulfides with the sign combination "−+−−−," resulted in significant changes in torsion angles across the disulfide bond. Except for 1kgc, in all other cases, at least two of five dihedral angles had changed by >40° on minimization. However, none of them converged to the "−−+−−" combination. The structures containing modeled disulfides in HB registered pairs on minimization showed significant changes in torsion angles across disulfide bonds. In all cases, at least one of the χ^1 angles underwent a change of >40° on minimization. None of the minimized structures adopt sign combination "−−+− −" observed for naturally occurring NHB cross-strand disulfides. The above observations confirm that "−−+−−" conformations for torsion angles, $\chi^1{}_i\chi^2{}_i\chi^{ss}\chi^2{}_j\chi^1{}_j$ are energetically preferred for disulfides at NHB registered pairs.

Further, energy minimizations were carried out for those proteins that were also studied experimentally in this work. The *in silico* introduced NHB cross-strand disulfides in proteins LBP and LIVBP converged to structures with torsion angle combinations $\chi^1{}_i\chi^2{}_i\chi^{ss}\chi^2{}_j\chi^1{}_j$ of "−−+−−" on minimization. The other NHB and HB disulfides in proteins MBP and Top7, however, adopted different combinations of torsion angles and are listed in Table SIII (Supporting Information). In general, there was no correlation between the stabilities of these mutants (described later) and the torsional angles predicted by the energy minimizations. This suggests that additional conformational sampling is required in addition to energy minimization.

Energy calculations for naturally occurring disulfides

As stated in earlier sections, in all the five naturally occurring HB cross-strand disulfides, the χ^1 values are very different from those of NHB cross-strand disulfides. This prompted us to check whether there are any steric clashes in HB registered pair cross-strand disulfides. The analysis showed that in all five of the HB cross-strand disulfides, the sulfur atom of at least one of the two cysteines involved in disulfide is close to either the main chain carbon or oxygen atoms of the same residue (S...C/O < 3.5 Å) (Table VII). A similar analysis was done for six randomly chosen NHB cross-strand disulfides. In none of the NHB cross-strand disulfides analyzed, the sulfur atom was close to the carbonyl group. This proximity between the sulfur atom and the cysteine carbonyl group might be one cause for the extremely rare occurrence of HB cross-strand disulfides. Energy calculations were carried out for the cystine moieties in the

Table VI
Stability of Top7 and Its Cross-Strand Disulfide Mutants as Measured by Isothermal Guanidinium Thiocyanate Denaturation Studies at 25°C, pH 8.0

Protein	Residues mutated to Cys: N-terminal residue (SA[a])	Residues mutated to Cys: C-terminal residue (SA[a])	Type of registered pair[b]	Side chain H-bonds[c]	ΔG^{0d} (25°C) (kcal/mol)	C_m[e] (M)	$\Delta\Delta G^{0f}$ (25°C) (kcal/mol)	$\Delta\Delta\Delta G^{0g}$ (25°C) (kcal/mol)	ΔC_m[h] (M)
Top7 WT					10.6 ± 1.7	3.3	—	—	—
Top7 Q5C T22C	Q5 (40.1)	T22 (60.9)	E-NHB	0	13.8 ± 1.8	4.1	3.2	3.9	0.8
Top7 S51C T89C[i]	S51 (21.8)	T89 (30.1)	E-NHB	1	>16.3 ± 0.1	>4.8	>5.7	>7.2	>1.5
Top7 V6C I52C	V6 (3.6)	I52 (1.1)	B-NHB	0	10.8 ± 0.1	3.4	0.2	2.5	0.1
Top7 V8C I50C[j]	V8 (2.4)	I50 (6.3)	B-NHB	0	24.8 ± 4.4	4.3	14.2	16.8	1.0
Top7 I10C I48C	I10 (3.1)	I48 (2.3)	B-NHB	0	9.4 ± 0.3	2.9	−1.2	0.8	−0.4
Top7 I4C V23C	I4 (15.8)	V23 (5.3)	E-HB	0	4.9 ± 0.2	1.5	−5.7	−4.4	−1.8
Top7 T82C T89C	T82 (28.9)	T89 (30.1)	E-HB	0	3.9 ± 0.2	1.2	−6.7	−4.5	−2.1
Top7 I50C V90C	I50 (6.3)	I90 (0.0)	B-HB	0	6.6 ± 0.2	2.1	−4.0	−1.5	−1.2
Top7 I52C V88C	I52 (1.1)	V88 (0.0)	B-HB	0	7.3 ± 0.1	2.3	−3.3	0.4	−1.0
Top7 Q5C T22C red[k]	Q5 (40.1)	T22 (60.9)	E-NHB	0	9.9 ± 0.1	3.0	−0.7	3.9	−0.3
Top7 S51C T89C red	S51 (21.8)	T89 (30.1)	E-NHB	1	9.1 ± 0.6	2.8	−1.5	>7.2	−0.5
Top7 V6C I52C red	V6 (3.6)	I52 (1.1)	B-NHB	0	8.3 ± 0.1	2.6	−2.3	2.5	−0.7
Top7 V8C I50C red	V8 (2.4)	I50 (6.3)	B-NHB	0	8.0 ± 0.3	2.3	−2.6	16.8	−1.0
Top7 I10C I48C red	I10 (3.1)	I48 (2.3)	B-NHB	0	8.6 ± 0.2	2.7	−2.0	0.8	−0.6
Top7 I4C V23C red	I4 (15.8)	V23 (5.3)	E-HB	0	9.3 ± 0.2	2.9	−1.3	−4.4	−0.4
Top7 T82C T89C red	T82 (28.9)	T89 (30.1)	E-HB	0	8.4 ± 0.2	2.6	−2.2	−4.5	−0.7
Top7 I50C V90C red	I50 (6.3)	I90 (0.0)	B-HB	0	8.1 ± 0.5	2.5	−2.5	−1.5	−0.8
Top7 I52C V88C red	I52 (1.1)	V88 (0.0)	B-HB	0	6.9 ± 0.1	2.1	−3.7	0.4	−1.2

[a]%Side chain accessibilities for WT residue are mentioned in parentheses.
[b]A mutant is referred to as exposed if at least one of the residues of the pair has side chain accessibility >7%. Types of registered pairs are E-NHB (exposed NHB), B-NHB (buried NHB), E-HB (exposed HB), and B-HB (buried HB).
[c]Number of hydrogen bonds formed by side chains of the WT residues.
[d]The m value used for fitting data for Top7 and all its mutants (except oxidized Top7 V8C I50C) in the oxidized and reduced states is -3.2 kcal mol^{-1} M^{-1}.
[e]Approximate error is 0.05M for C_m.
[f]$\Delta\Delta G^0 = \Delta G^0$(mutant) $- \Delta G^0$(WT) where ΔG^0 is free energy of unfolding.
[g]$\Delta\Delta\Delta G^0 = \Delta\Delta G^0$(oxidized) $- \Delta\Delta G^0$ (reduced).
[h]$\Delta C_m = C_m$(mutant) $- C_m$(WT), where C_m is the concentration of denaturant at which 50% protein is unfolded.
[i]No unfolded baseline was obtained for fitting data of Top7 S51C T89C. Approximate unfolding parameters were derived from a two-state fit obtained by assuming the protein to be completely unfolded at [Gdm SCN] $\geq$ 5.4M [Fig. 7(A)].
[j]The unfolding of oxidized Top7 V8C I50C was fit with an m-value of -5.8 kcal mol^{-1} M^{-1}.
[k]All melts in the reduced state were carried out in the presence of 20-fold molar excess of DTT.

above mentioned proteins on GROMACS 3.3.3. The Lennard–Jones potential energies for the residues forming the disulfides were computed and compared (Table VII). Three HB cross-strand disulfides have positive energy values, whereas two have negative energy values. All the NHB cross-strand disulfides studied have negative Lennard–Jones potential energies that are typically lower than those found for the HB cross-strand disulfides.

Frequency of occurrence of cross-strand disulfides

Of the 2311 naturally occurring disulfides in the nonredundant data set, only 76 are cross-strand disulfides. This led us to the question whether cross-strand disulfides are particularly difficult to accommodate in antiparallel β-sheets. Further previous studies have indicated that these disulfides are rare and are highly strained.[7,8,12] MODIP predicts residue pairs that are in proximity and in the right orientation to accommodate disulfides. Hence, we used MODIP to predict disulfide introduction sites in the entire protein data set and in the antiparallel β-sheets. There were 201,984 sites predicted in the entire nonredundant protein data set containing 2311 naturally occurring disulfides. There were 7795 sites predicted for the nonredundant data set of

Table VII
Comparison of Lennard–Jones Potential Energies of Naturally Occurring Cross-Strand Disulfides at HB and NHB Positions

PDB ID	Pair type	Cys_i–Cys_j	Distance (Å): S_i–C_i	S_i–O_i	S_j–C_j	S_j–O_j	Lennard–Jones potential energy[a] (kJ/mol)
1ahk	HB	8–119	4.05	4.43	**2.71**[b]	3.38	1.0
1ahm	HB	8–119	3.89	4.32	**2.87**	3.65	0.8
1b56	HB	120–127	3.30	3.43	**2.91**	3.19	−0.2
1hre	HB	182–196	4.18	5.18	3.29	3.97	2.5
1hrf	HB	182–196	4.14	5.01	3.35	4.14	−0.1
1elt	NHB	136–201	4.94	4.18	4.84	4.15	−5.6
1f94	NHB	6–11	4.84	3.14	4.53	3.22	−7.2
1noa	NHB	37–47	4.91	4.13	5.03	4.15	−3.9
1nsc	NHB	230–235	4.14	4.75	4.17	4.83	−3.2
1uze	NHB	152–158	4.17	4.88	4.18	4.83	−5.0
2bw8	NHB	66–71	4.65	4.15	4.82	4.13	−0.2

[a]After excluding (1,2), (1,3), and (1,4) interactions, the Lennard–Jones potential energies were calculated and summed up for all possible pairs of atoms constituting the cystine moiety using GROMACS 3.3.3 package.
[b]The distance values less than 3.0 Å are in bold.

antiparallel β-sheets containing 76 naturally occurring disulfides. Hence, the ratios of observed disulfides to stereochemically compatible sites are 1.1% and 1.0% for the entire data set and antiparallel β-strands, respectively. This demonstrates that cross-strand disulfides are not particularly rare and are unlikely to be strained.

Oxidation status of cross-strand disulfide mutants

To experimentally study requirements for cross-strand disulfide formation, pairs of CYS residues were introduced at NHB and HB positions (Tables V and VI). A registered pair is considered exposed if at least one residue of the pair has side chain accessibility >7%.[58] All HB pairs chosen were such that the main chain atoms of the registered pair formed two hydrogen bonds between them. All mutants (except Top7 Q5C T22C) were generated by mutating residues that were not involved in any hydrogen bonding through their side chains.[33] The residues Gln 5 and Thr 22 in Top7 are involved in hydrogen bonding with each other through their side chains.

The oxidation status of all the purified proteins was checked by mass spectroscopy before and after incubation with iodoacetamide. If a disulfide is formed, there is no change in mass after incubation with iodoacetamide. In the absence of disulfide formation, each free CYS residue will react with iodoacetamide, resulting in a mass increase of 58.0 Da per CYS.

All the mutants made in the proteins MBP, LBP, and LIVBP were at NHB registered pairs. Most residues in the β-sheets of these proteins are buried. No cysteines were introduced in HB registered pairs because it was not possible to do so without disrupting several preformed side-chain interactions. In the above three proteins, only one mutant of LBP (LBP L245C Q335C) was at an exposed NHB registered pair, whereas all remaining mutants were at buried NHB positions. All mutants except LIVBP T247C V331C showed disulfide formation after purification.

Top7, a designed protein,[40] was another system chosen to study the effects of cross-strand disulfides owing to its high stability and a well-formed relatively flat five-stranded β-sheet. The sequence of WT Top7 used in this work is indicated in the footnote of Table SIII (Supporting Information). In the two exposed Top7 NHB mutants (Top7 Q5C T22C and Top7 S51C T89C) and one buried NHB mutant (Top7 I10C I48C), disulfide formation was observed after purification. Two other buried NHB mutants (Top7 V6C I52C and Top7 V8C I50C) had to be subjected to stronger oxidizing conditions with copper-phenanthroline to facilitate disulfide formation. One of the two exposed Top7 HB mutants (Top7 T82C T89C) showed disulfide formation on purification. The other exposed HB mutant Top7 I4C V23C and the buried HB mutants (Top7 I50C V90C and Top7 I52C V88C) had to be treated with oxidizing agents to aid disulfide formation.

The above observations indicate that disulfides introduced at exposed NHB positions form with greater ease than at other registered pair positions in antiparallel β-strands. Although HB registered pair disulfides are not observed in naturally occurring proteins, they were observed to form in the above engineered proteins, though, typically, formation required the addition of the copper-phenanthroline oxidizing agent.

Far UV CD spectra

The far UV CD spectra were collected for all the purified proteins in the wavelength range of 200–250 nm in the oxidized and reduced states (Fig. 5) and compared with corresponding spectra for the WT protein. All mutants except Top7 V8C I50C (in oxidized and reduced states) and reduced Top7 I52C V88C displayed far UV CD spectra similar to that of the corresponding WT in both oxidized and reduced states. This indicates that the introduction of disulfide has not altered the structure drastically.

Chemical denaturation studies

Chemical denaturation studies were carried out with urea for LBP and MBP mutants in both oxidized and reduced states (Table V). ΔG^0 refers to the free energy change on unfolding of the protein. $\Delta\Delta G^0 = \Delta G^0(\text{mutant}) - \Delta G^0(\text{WT})$ is the stability of the mutant relative to WT. $\Delta\Delta\Delta G^0 = \Delta\Delta G^0(\text{ox}) - \Delta\Delta G^0(\text{red})$ is the contribution of disulfide bond formation to stability. The introduction of a disulfide in both the exposed NHB LBP mutant (LBP L245C Q335C) and the buried NHB mutant (LBP T247C V333C) destabilized the protein by 2.1–2.9 kcal/mol relative to WT LBP. WT LBP has a naturally occurring disulfide. The value of $\Delta\Delta\Delta G^0$ is zero for the mutant LBP L245C Q335C. This indicates that the formation of a disulfide between 245 and 335 positions does not confer any change in stability toward denaturation by urea. The loss of stability in the oxidized state is presumably because of loss of favorable interactions involving residues L245 and Q335 on mutation. The formation of disulfide in the other LBP mutant LBP T247C V333C was also destabilizing with respect to the WT LBP. The reduced state of this mutant was highly destabilized. The reduced mutant lacked a folded baseline in the denaturation profile. The data for this mutant, therefore, imply that introduction of the disulfide has significantly stabilized the protein, relative to the reduced state. The LIVBP mutant was not studied because this protein could not be obtained in the completely oxidized form.

The buried NHB mutant MBP V110C V261C was destabilized with respect to WT MBP in the oxidized state ($\Delta C_m = -0.2M$). WT MBP has no disulfides. The corresponding chemical melt carried out in the reduced

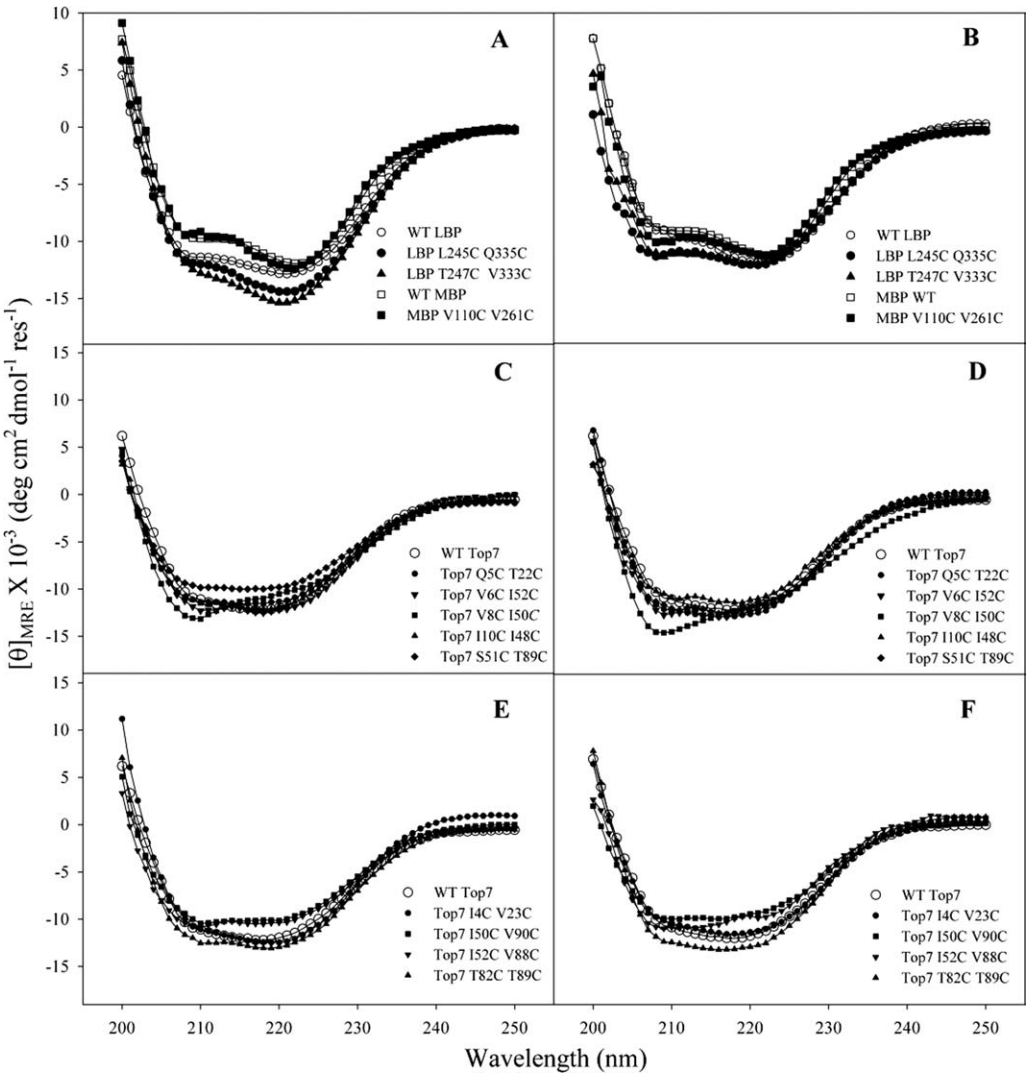

Figure 5

Far UV CD spectra of (**A**) oxidized WT LBP, oxidized LBP L245C Q335C, oxidized LBP T247C V333C, WT MBP, and oxidized MBP V110 V261C; (**B**) reduced WT LBP, reduced LBP L245C Q335C, reduced LBP T247C V333C, WT MBP, and reduced MBP V110 V261C; (**C**) WT Top7 and Top7 NHB mutants in oxidized state; (**D**) WT Top7 and Top7 NHB mutants in reduced state; (**E**) WT Top7 and Top7 HB mutants in oxidized state; and (**F**) WT Top7 and Top7 HB mutants in reduced state.

state for the mutant showed that it was further destabilized with respect to the oxidized state, indicating that the disulfide is stabilizing in this NHB position ($\Delta\Delta\Delta G^0$ = 3.0 kcal/mol).

Top7 is a highly stable protein lacking disulfides and is resistant to urea denaturation. Therefore, a stronger denaturant, Gdm SCN was used to study the stability of Top7 and its mutants. At 25°C, pH 8.0, WT Top 7 has values of ΔG^0 and C_m of 10.6 kcal/mol and 3.3*M*, respectively, with this denaturant (Table VI). A total of nine Top7 mutants were made and studied; five at NHB pairs and four at HB pairs (Table VI). The two Top7 mutants, Top7 Q5C T 22C and Top7 S51C T89C in exposed NHB positions were stabilized in the oxidized state with respect to WT Top7. The C_m for Top7 Q5C T22C is 0.8*M* greater than that for WT Top7. The mutant Top7 S51C T89C was stabilized in the oxidized state to such an extent that the protein was not completely unfolded at the highest concentration of denaturant that was used (5.4*M* Gdm SCN). The comparison of stabilities of the oxidized proteins with those in the reduced state revealed that the disulfide was stabilizing in both exposed NHB mutants.

The buried NHB position mutants, Top7 V6C I52C, Top7 V8C I50C, and Top7 I10C I48C have C_m values of 3.4, 4.3, and 2.9*M* in the oxidized and 2.6, 2.3, and 2.7*M* in the reduced state, respectively, whereas WT Top7 has a C_m value of 3.3*M*. Thus, disulfide formation in all three cases is stabilizing ($\Delta\Delta\Delta G^0 > 0$). The C_m of Top7 V8C I50C in the oxidized state is 1*M* greater than WT Top7.

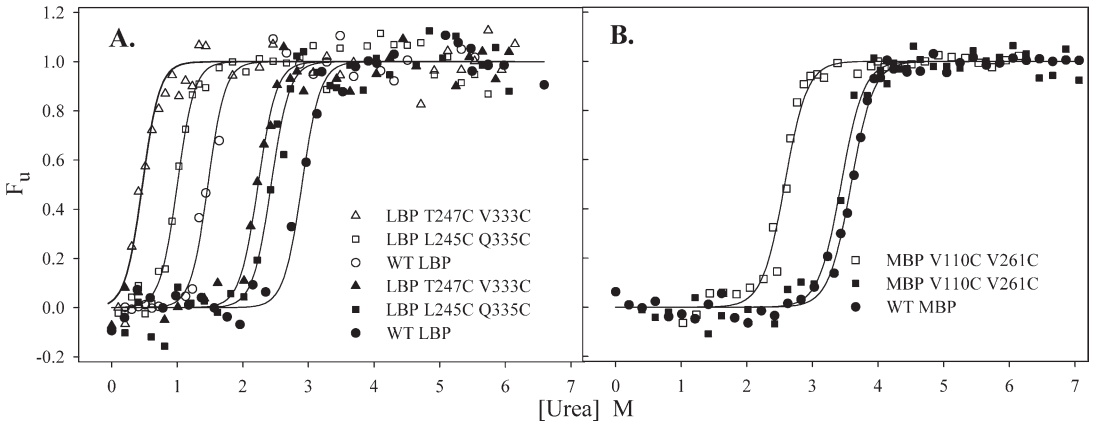

Figure 6

Urea chemical denaturation studies carried out at 25°C for oxidized and reduced states of (**A**) LBP L245C Q335C, LBP T247C V333C, and LBP WT and (**B**) MBP V110C V261C and MBP WT. In each of the plots, the melt profile for oxidized type is represented by filled symbols, whereas those for reduced state are represented by open symbols. The continuous lines in all plots represent the fits for two-state unfolding model. The data for WT LBP and LBP mutants were fitted to a two-state model using *m*-values of −4.2 and −4.5 kcal mol^{-1} M^{-1} in the oxidized state and reduced state, respectively. The data for MBP and MBP V110C V261C were fitted to a two-state model with *m*-value of −3.4 kcal mol^{-1} M^{-1}. The mutant LBP T247C V333C in its reduced state did not display a folded baseline on chemical denaturation owing to destabilization. An approximate two-state fit for this reduced mutant was obtained by using the slope and intercept values of the folded baseline of reduced LBP WT.

However, the slope for the unfolding transition of this protein in the oxidized state (m = −5.8 kcal mol^{-1} M^{-1}) is very different from that for WT Top7 (m = −3.2 kcal mol^{-1} M^{-1}). It must also be noted, as previously discussed, that this mutant also displayed a secondary CD spectrum that is different from that of WT. Because both the residues mutated to cysteines in this mutant are buried in the WT structure, it is likely that disulfide formation in this mutant has resulted in a structure that is different from that of the WT. Further, disulfide introduction might also result in structural changes in the denatured state. The *m*-value is related to the amount of surface area buried on unfolding[59] and structural features of the denatured state also can affect the *m*-value of unfolding of proteins.[60] Introduction of a disulfide would normally be expected to decrease the accessible surface of the unfolded state and, hence, decrease the magnitude of the *m*-value. The large increase in *m*-value is therefore surprising. In contrast, the unfolding transition of the reduced Top7 V8C I50C protein can be fitted with the same slope as WT Top7. Regardless of this issue, this mutant is significantly stabilized with respect to WT, though interpretation of the data is complicated by changes in the *m*-value and CD spectra.

The two exposed HB mutants, Top7 I4C V23C and Top7 T82C T89C, are both destabilized relative to WT with ΔC_m values of −1.8M and −2.1M, respectively. Unlike the Top7 NHB mutants, the ΔG^0 of these mutants increased when the disulfide was reduced ($\Delta\Delta G^0$ values of −4.4 and −4.5 kcal/mol, respectively). The reduction of the disulfide in both Top7 I4C V23C and Top7 T82C T89C led to an increase in C_m by 1.4M relative to their corresponding oxidized states. This indicates that disulfide formation at both these HB positions destabilizes the protein.

The two buried HB mutants, Top7 I50C V90C and Top7 I52C V88C, have reduced C_m values of 2.1M and 2.3M, respectively, with respect to 3.3M for WT Top7. A comparison of stabilities of these proteins in the oxidized and reduced states shows that Top7 I50C V90C was more stable in the reduced state ($\Delta\Delta\Delta G^0$ = −1.5M), whereas Top7 I52C V88C was less stable in the reduced state ($\Delta\Delta\Delta G^0$ = 0.4M). Top7 I52C V88C is the only HB disulfide mutant in this study that has a nondestabilizing disulfide, that is, where $\Delta\Delta\Delta G^0 > 0$. The results are summarized in Tables V and VI and Figures 6 and 7.

Thermal denaturation studies

Thermal denaturation studies were carried out for the oxidized proteins of WT LBP, LBP mutants, WT MBP, and MBP mutant (Table V and Fig. 8). Thermal melts could not be carried out with reduced proteins because of complications involving oxidation during denaturation and irreversibility of the transitions. Top7 and its mutants are highly stable and are resistant to thermal denaturation even at 100°C. Hence, no thermal stability studies were carried out with Top7 and its mutants. Although the thermal denaturation data of WT LBP and WT MBP could be fit to a two-state unfolding model, those of LBP mutants and MBP mutant could not be fit to a two-state model. However, the differential scanning calorimetry data were used as a basis for comparison of stabilities in terms of transition temperature values. The

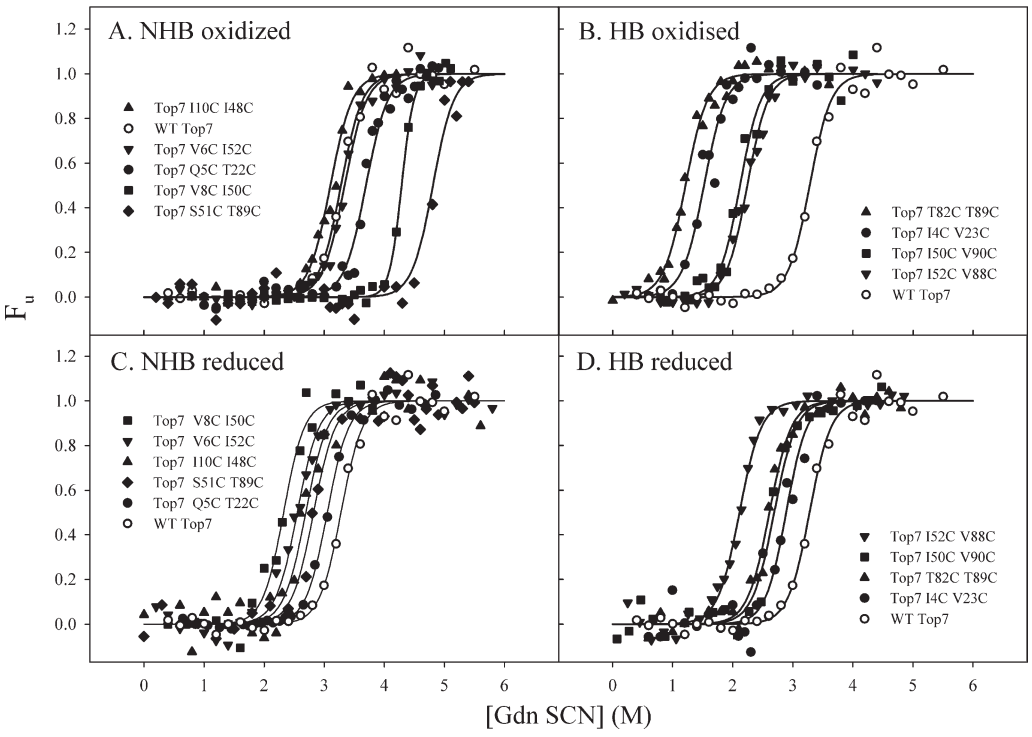

Figure 7

Gdm SCN chemical denaturation studies carried out at 25°C for (**A**) oxidized NHB mutants, (**B**) oxidized HB mutants, (**C**) reduced NHB mutants, and (**D**) reduced HB mutants. The plot for WT Top7 is also provided in each of the panels. All data were fitted to a two-state unfolding model. The *m*-value used for the fits in all cases except oxidized Top7 V8C I I50C was -3.2 kcal mol^{-1} M^{-1}. The data for oxidized Top7 V8C I I50C were fit to a two-state model with *m*-value of -5.8 kcal mol^{-1} M^{-1}. The mutant Top7 S51C T89C was highly stabilized and did not undergo complete denaturation. An approximate two-state fit was obtained by assuming the protein to be completely unfolded at [Gdm SCN] $> 5.4M$.

exposed NHB disulfide mutant LBP L245C Q335C is more stable than WT LBP ($\Delta T_m = 3.1$°C). However, the buried NHB mutant LBP T247C V333C is less stable than WT LBP ($\Delta T_m = -1.6$°C). The buried NHB mutant, MBP V110C V261C is destabilized with respect to WT MBP ($\Delta T_m = -1.2$°C).

The thermal denaturation studies showed that the only NHB mutant studied that displayed an increase in stability with respect to WT was an exposed one. This further confirms that the chances of engineering a stabilizing disulfide in a β-sheet are high if the chosen site is an exposed NHB registered pair.

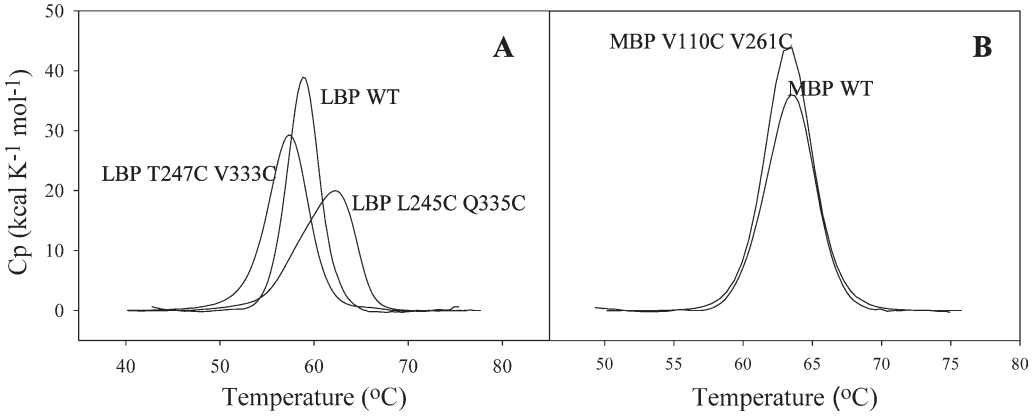

Figure 8

Baseline subtracted differential scanning calorimetry scans for (**A**) NHB disulfide bonded mutants of LBP and (**B**) MBP. The plots for WT LBP and WT MBP are included for comparison. Protein identities are indicated in the plots.

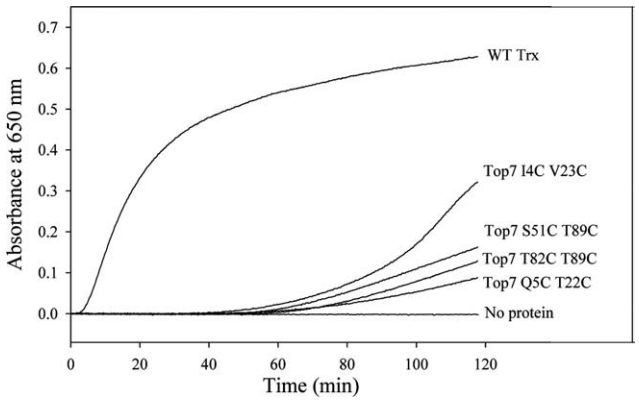

Figure 9

Insulin reduction assay for redox activity. Insulin aggregation following reduction was monitored by the increase in light scattering at 650 nm. Assay conditions were 0.1*M* phosphate buffer, 2 m*M* EDTA, 0.13 m*M* porcine insulin, 0.33 m*M* DTT, and 10 μ*M* protein. Protein identities are adjacent to each trace. Incubation mixture without protein served as negative control and WT Trx served as a positive control.

Redox activity of engineered cross-strand disulfide mutants in Top7

Cross-strand disulfides are believed to play a role as redox switches in several proteins of varied functions.[13] A redox sensor that undergoes change in its fluorescence properties in response to its redox environment has been engineered by introducing a disulfide in the registered pair of the β-barrel of green fluorescent protein.[61] Hence, we examined the engineered cross-strand disulfides for redox activity through the insulin reduction assay. The four exposed Top7 mutants, Top7 I4C V23C, Top7 Q5C T22C, Top7 S51C T89C, and Top7 T82C T89C, were checked for redox activity. All four Top7 mutants showed varying levels of activity (Fig. 9). There is no correlation between the nature of cross-strand disulfides and level of activity. Both HB and NHB cross-strand disulfides show redox activity. However, all of them were less active than the positive control, WT Trx. This is expected because WT Trx is evolutionarily optimized for redox activity. Previous experiments done with MBP 230C 30C and nSS Trx 20C 73C (lacking the disulfide present in WT Trx) showed that they are redox inactive.[5] The C^{α} atoms of residues 230 and 30 in WT MBP, and residues 20 and 73 in WT Trx are separated by 35.3 Å and 27.3 Å, respectively. The inactivity of these mutants shows that mere presence of two cysteines in a protein does not confer redox activity. The introduction of cross-strand disulfides can, thus, be used to engineer redox activity.

CONCLUSIONS

Our studies have shown that in antiparallel strands, engineered disulfides at exposed NHB registered pairs provide a robust means of increasing protein stability. Given the previous difficulties with design of stabilizing disulfides, this is an encouraging result. Such engineered disulfides may provide a general method for stabilizing β-rich proteins. Engineered cross-strand disulfides may also be a useful strategy to rigidify β-strands in peptide models of antiparallel β-sheets.[62,63] In addition, we have rationalized the preference of cross-strand disulfides for NHB relative to HB positions. We also found no evidence to suggest that the cross-strand disulfides are strained. Experimental studies with the proteins LBP, MBP, and Top7 have shown that disulfides can be introduced at both NHB and HB registered pairs. The disulfides at buried NHB sites are also stabilizing in nature ($\Delta\Delta\Delta G^0 > 0$). However, the stabilizing effect of these disulfides is often masked by the destabilization effects owing to loss of native interactions upon mutation. The disulfides at HB registered pairs are destabilizing and often do not form in the absence of an external oxidizing agent. The formation and effect of cross-strand disulfides on protein stabilities could be used as a tool to determine the registry in antiparallel sheets of proteins of unknown structure. Introduction of cross-strand disulfides can also be used to engineer redox activity.

ACKNOWLEDGMENTS

C.R. is a senior Scientist of the Indian National Science Academy. The authors thank Prof. David Baker for providing the Top7 construct. Bharat Adkar and M. S. Vijay Bhaskar are thanked for helpful discussions.

REFERENCES

1. Creighton TE. Disulphide bonds and protein stability. Bioessays 1988;8:57–63.
2. Harrison PM, Sternberg MJ. Analysis and classification of disulphide connectivity in proteins. The entropic effect of cross-linkage. J Mol Biol 1994;244:448–463.
3. Ladbury JE, Kishore N, Hellinga HW, Wynn R, Sturtevant JM. Thermodynamic effects of reduction of the active-site disulfide of *Escherichia coli* thioredoxin explored by differential scanning calorimetry. Biochemistry 1994;33:3688–3692.
4. Pace CN, Grimsley GR, Thomson JA, Barnett BJ. Conformational stability and activity of ribonuclease T1 with zero, one, and two intact disulfide bonds. J Biol Chem 1988;263:11820–11825.
5. Indu S, Kumar ST, Thakurela S, Gupta M, Bhaskara RM, Ramakrishnan C, Varadarajan R. Disulfide conformation and design at helix N-termini. Proteins 2010;78:1228–1242.
6. Chakraborty K, Thakurela S, Prajapati RS, Indu S, Ali PS, Ramakrishnan C, Varadarajan R. Protein stabilization by introduction of cross-strand disulfides. Biochemistry 2005;44:14638–14646.
7. Thornton JM. Disulphide bridges in globular proteins. J Mol Biol 1981;151:261–287.
8. Richardson JS. The anatomy and taxonomy of protein structure. Adv Protein Chem 1981;34:167–339.
9. Harrison PM, Sternberg MJ. The disulphide beta-cross: from cystine geometry and clustering to classification of small disulphide-rich protein folds. J Mol Biol 1996;264:603–623.
10. Wouters MA, Curmi PM. An analysis of side chain interactions and pair correlations within antiparallel beta-sheets: the differences

between backbone hydrogen-bonded and non-hydrogen-bonded residue pairs. Proteins 1995;22:119–131.
11. Haworth NL, Feng LL, Wouters MA. High torsional energy disulfides: relationship between cross-strand disulfides and right-handed staples. J Bioinform Comput Biol 2006;4:155–168.
12. Wouters MA, George RA, Haworth NL. "Forbidden" disulfides: their role as redox switches. Curr Protein Pept Sci 2007;8:484–495.
13. Wouters MA, Lau KK, Hogg PJ. Cross-strand disulphides in cell entry proteins: poised to act. Bioessays 2004;26:73–79.
14. Schmidt B, Ho L, Hogg PJ. Allosteric disulfide bonds. Biochemistry 2006;45:7429–7433.
15. Chivers PT, Prehoda KE, Raines RT. The CXXC motif: a rheostat in the active site. Biochemistry 1997;36:4061–4066.
16. Yang Y, Song Y, Loscalzo J. Regulation of the protein disulfide proteome by mitochondria in mammalian cells. Proc Natl Acad Sci U S A 2007;104:10813–10817.
17. Hausman SZ, Manclark CR, Burns DL. Binding of ATP by pertussis toxin and isolated toxin subunits. Biochemistry 1990;29:6128–6131.
18. Stenmark H, Olsnes S, Madshus IH. Elimination of the disulphide bridge in fragment B of diphtheria toxin: effect on membrane insertion, channel formation, and ATP binding. Mol Microbiol 1991;5:595–606.
19. Erdal E, Bartels F, Binscheck T, Erdmann G, Frevert J, Kistner A, Weller U, Wever J, Bigalke H. Processing of tetanus and botulinum A neurotoxins in isolated chromaffin cells. Naunyn Schmiedebergs Arch Pharmacol 1995;351:67–78.
20. Toyoda T, Gotoh B, Sakaguchi T, Kida H, Nagai Y. Identification of amino acids relevant to three antigenic determinants on the fusion protein of Newcastle disease virus that are involved in fusion inhibition and neutralization. J Virol 1988;62:4427–4430.
21. Yusoff K, Nesbit M, McCartney H, Meulemans G, Alexander DJ, Collins MS, Emmerson PT, Samson AC. Location of neutralizing epitopes on the fusion protein of Newcastle disease virus strain Beaudette C. J Gen Virol 1989;70(Pt 11):3105–3109.
22. Jain S, McGinnes LW, Morrison TG. Thiol/disulfide exchange is required for membrane fusion directed by the Newcastle disease virus fusion protein. J Virol 2007;81:2328–2339.
23. Rosenthal PB, Zhang X, Formanowski F, Fitz W, Wong CH, Meier-Ewert H, Skehel JJ, Wiley DC. Structure of the haemagglutinin-esterase-fusion glycoprotein of influenza C virus. Nature 1998;396:92–96.
24. Barbouche R, Miquelis R, Jones IM, Fenouillet E. Protein-disulfide isomerase-mediated reduction of two disulfide bonds of HIV envelope glycoprotein 120 occurs post-CXCR4 binding and is required for fusion. J Biol Chem 2003;278:3131–3136.
25. Matthias LJ, Yam PT, Jiang XM, Vandegraaff N, Li P, Poumbourios P, Donoghue N, Hogg PJ. Disulfide exchange in domain 2 of CD4 is required for entry of HIV-1. Nat Immunol 2002;3:727–732.
26. Jacob-Dubuisson F, Pinkner J, Xu Z, Striker R, Padmanhaban A, Hultgren SJ. PapD chaperone function in pilus biogenesis depends on oxidant and chaperone-like activities of DsbA. Proc Natl Acad Sci U S A 1994;91:11552–11556.
27. Ahamed J, Versteeg HH, Kerver M, Chen VM, Mueller BM, Hogg PJ, Ruf W. Disulfide isomerization switches tissue factor from coagulation to cell signaling. Proc Natl Acad Sci U S A 2006;103:13932–13937.
28. Goulding CW, Sawaya MR, Parseghian A, Lim V, Eisenberg D, Missiakas D. Thiol-disulfide exchange in an immunoglobulin-like fold: structure of the N-terminal domain of DsbD. Biochemistry 2002;41:6920–6927.
29. Dani VS, Ramakrishnan C, Varadarajan R. MODIP revisited: re-evaluation and refinement of an automated procedure for modeling of disulfide bonds in proteins. Protein Eng 2003;16:187–193.
30. Sowdhamini R, Srinivasan N, Shoichet B, Santi DV, Ramakrishnan C, Balaram P. Stereochemical modeling of disulfide bridges. Criteria for introduction into proteins by site-directed mutagenesis. Protein Eng 1989;3:95–103.
31. Guex N, Peitsch MC. SWISS-MODEL and the Swiss-PdbViewer: an environment for comparative protein modeling. Electrophoresis 1997;18:2714–2723.
32. Lindahl EHB, van der Spoel D. GROMACS 3.0: a package for molecular simulation and trajectory analysis. J Mol Model 2001;7:306–317.
33. McDonald IK, Thornton JM. Satisfying hydrogen bonding potential in proteins. J Mol Biol 1994;238:777–793.
34. Ho SN, Hunt HD, Horton RM, Pullen JK, Pease LR. Site-directed mutagenesis by overlap extension using the polymerase chain reaction. Gene 1989;77:51–59.
35. Beena K, Udgaonkar JB, Varadarajan R. Effect of signal peptide on the stability and folding kinetics of maltose binding protein. Biochemistry 2004;43:3608–3619.
36. Ganesh C, Shah AN, Swaminathan CP, Surolia A, Varadarajan R. Thermodynamic characterization of the reversible, two-state unfolding of maltose binding protein, a large two-domain protein. Biochemistry 1997;36:5020–5028.
37. Magnusson U, Salopek-Sondi B, Luck LA, Mowbray SL. X-ray structures of the leucine-binding protein illustrate conformational changes and the basis of ligand specificity. J Biol Chem 2004;279:8747–8752.
38. Prajapati RS, Sirajuddin M, Durani V, Sreeramulu S, Varadarajan R. Contribution of cation-pi interactions to protein stability. Biochemistry 2006;45:15000–15010.
39. Prajapati RS, Indu S, Varadarajan R. Identification and thermodynamic characterization of molten globule states of periplasmic binding proteins. Biochemistry 2007;46:10339–10352.
40. Kuhlman B, Dantas G, Ireton GC, Varani G, Stoddard BL, Baker D. Design of a novel globular protein fold with atomic-level accuracy. Science 2003;302:1364–1368.
41. Pace CN, Vajdos F, Fee L, Grimsley G, Gray T. How to measure and predict the molar absorption coefficient of a protein. Protein Sci 1995;4:2411–2423.
42. Careaga CL, Falke JJ. Thermal motions of surface alpha-helices in the D-galactose chemosensory receptor. Detection by disulfide trapping. J Mol Biol 1992;226:1219–1235.
43. Creighton TE. Counting integral numbers of amino acid residues per polypeptide chain. Nature 1980;284:487–489.
44. Kelley RF, Shalongo W, Jagannadham MV, Stellwagen E. Equilibrium and kinetic measurements of the conformational transition of reduced thioredoxin. Biochemistry 1987;26:1406–1411.
45. Holmgren A. Thioredoxin catalyzes the reduction of insulin disulfides by dithiothreitol and dihydrolipoamide. J Biol Chem 1979;254:9627–9632.
46. Murzin AG, Brenner SE, Hubbard T, Chothia C. SCOP: a structural classification of proteins database for the investigation of sequences and structures. J Mol Biol 1995;247:536–540.
47. Burmeister WP, Henrissat B, Bosso C, Cusack S, Ruigrok RW. Influenza B virus neuraminidase can synthesize its own inhibitor. Structure 1993;1:19–26.
48. Crennell S, Takimoto T, Portner A, Taylor G. Crystal structure of the multifunctional paramyxovirus hemagglutinin-neuraminidase. Nat Struct Biol 2000;7:1068–1074.
49. Lawrence MC, Borg NA, Streltsov VA, Pilling PA, Epa VC, Varghese JN, McKimm-Breschkin JL, Colman PM. Structure of the haemagglutinin-neuraminidase from human parainfluenza virus type III. J Mol Biol 2004;335:1343–1357.
50. Smith BJ, Colman PM, Von Itzstein M, Danylec B, Varghese JN. Analysis of inhibitor binding in influenza virus neuraminidase. Protein Sci 2001;10:689–696.
51. Modis Y, Ogata S, Clements D, Harrison SC. Structure of the dengue virus envelope protein after membrane fusion. Nature 2004;427:313–319.
52. Rey FA, Heinz FX, Mandl C, Kunz C, Harrison SC. The envelope glycoprotein from tick-borne encephalitis virus at 2 A resolution. Nature 1995;375:291–298.

53. Bravo J, Staunton D, Heath JK, Jones EY. Crystal structure of a cytokine-binding region of gp130. EMBO J 1998;17:1665–1674.
54. Syed RS, Reid SW, Li C, Cheetham JC, Aoki KH, Liu B, Zhan H, Osslund TD, Chirino AJ, Zhang J, Finer-Moore J, Elliott S, Sitney K, Katz BA, Matthews DJ, Wendoloski JJ, Egrie J, Stroud RM. Efficiency of signalling through cytokine receptors depends critically on receptor orientation. Nature 1998;395:511–516.
55. Teplyakov A, Obmolova G, Wilson K, Kuromizu K. Crystal structure of apo-neocarzinostatin at 0.15-nm resolution. Eur J Biochem 1993;213:737–741.
56. Kuroki K, Tsuchiya N, Shiroishi M, Rasubala L, Yamashita Y, Matsuta K, Fukazawa T, Kusaoi M, Murakami Y, Takiguchi M, Juji T, Hashimoto H, Kohda D, Maenaka K, Tokunaga K. Extensive polymorphisms of LILRB1 (ILT2. LIR1) and their association with HLA-DRB1 shared epitope negative rheumatoid arthritis. Hum Mol Genet 2005;14:2469–2480.
57. Love CA, Harlos K, Mavaddat N, Davis SJ, Stuart DI, Jones EY, Esnouf RM. The ligand-binding face of the semaphorins revealed by the high-resolution crystal structure of SEMA4D. Nat Struct Biol 2003;10:843–848.
58. Lee B, Richards FM. The interpretation of protein structures: estimation of static accessibility. J Mol Biol 1971;55: 379–400.
59. Myers JK, Pace CN, Scholtz JM. Denaturant m values and heat capacity changes: relation to changes in accessible surface areas of protein unfolding. Protein Sci 1995;4:2138–2148.
60. Wrabl J, Shortle D. A model of the changes in denatured state structure underlying m value effects in staphylococcal nuclease. Nat Struct Biol 1999;6:876–883.
61. Hanson GT, Aggeler R, Oglesbee D, Cannon M, Capaldi RA, Tsien RY, Remington SJ. Investigating mitochondrial redox potential with redox-sensitive green fluorescent protein indicators. J Biol Chem 2004;279:13044–13053.
62. Chakraborty K, Shivakumar P, Raghothama S, Varadarajan R. NMR structural analysis of a peptide mimic of the bridging sheet of HIV-1 gp120 in methanol and water. Biochem J 2005;390: 573–581.
63. Kier BL, Shu I, Eidenschink LA, Andersen NH. Stabilizing capping motif for beta-hairpins and sheets. Proc Natl Acad Sci U S A 2010;107:10466–10471.